# A new source of methylglyoxal in the aqueous phase

Maria Rodigast, Anke Mutzel, Janine Schindelka and Hartmut Herrmann*

*Leibniz Institute for Tropospheric Research (TROPOS), Atmospheric Chemistry Dept. (ACD), Permoserstr. 15, D-04318 Leipzig, Germany*

*Corresponding author. Tel: +49-341-2717-7024; fax: +49-341-271799-7024.

*E-mail address:* herrmann@tropos.de

1 **Abstract**
2 Carbonyl compounds are ubiquitous in atmospheric multiphase system participating in gas, particle, and aqueous-
3 phase chemistry. One important compound is methyl ethyl ketone (MEK), as it is detected in significant amounts
4 in the gas phase as well as in cloud water, ice, and rain. Consequently, it can be expected that MEK influences the
5 liquid phase chemistry. Therefore, the oxidation of MEK and the formation of corresponding oxidation products
6 were investigated in the aqueous phase. Several oxidation products were identified from the oxidation with OH
7 radicals, including 2,3-butanedione, hydroxyacetone, and methylglyoxal. The molar yields were 29.5% for
8 2,3-butanedione, 3.0% for hydroxyacetone, and 9.5% for methylglyoxal. Since methylglyoxal is often related to
9 the formation of organics in the aqueous phase, MEK should be considered for the formation of aqueous secondary
10 organic aerosol (aqSOA). Based on the experimentally obtained data, a reaction mechanism for the formation of
11 methylglyoxal has been developed and evaluated with a model study. Besides known rate constants, the model
12 contains measured photolysis rate constants for MEK ($k_p = 5 \times 10^{-5}$ s$^{-1}$), 2,3-butanedione ($k_p = 9 \times 10^{-6}$ s$^{-1}$),
13 methylglyoxal ($k_p = 3 \times 10^{-5}$ s$^{-1}$), and hydroxyacetone ($k_p = 2 \times 10^{-5}$ s$^{-1}$). From the model predictions, a branching
14 ratio of 60/40 for primary/secondary H-atom abstraction at the MEK skeleton was found. This branching ratio
15 reproduces the experiment results very well, especially the methylglyoxal formation, which showed excellent
16 agreement. Overall, this study demonstrates MEK as a methylglyoxal precursor compound for the first time.
17

## 1. Introduction

In the last decades, carbonyl compounds have been a subject of intense research due to their ubiquitous abundance and their effect on atmospheric chemistry and human health. They are emitted directly from biogenic and anthropogenic sources or formed through the oxidation of hydrocarbons (e.g., Atkinson, 1997; Matthews and Howell, 1981; Lipari et al., 1984; Ciccioli et al., 1993; Mopper and Stahovec, 1986; Carlier et al., 1986; Hallquist et al., 2009). One carbonyl compound that is emitted from numerous and mainly biological sources is methyl ethyl ketone (MEK). It is released from grass, clover (Kirstine et al., 1998; de Gouw et al., 1999), different types of forests, and biomass burning processes (Khalil and Rasmussen, 1992; Warneke et al., 1999; Isidorov et al., 1985). Anthropogenic emissions are also important MEK sources, such as artificial biomass burning (Andreae and Merlet, 2001; Akagi et al., 2011; Yokelson et al., 2013; Brilli et al., 2014) and tobacco smoke (Buyske et al., 1956; Yokelson et al., 2013). In addition, MEK is emitted into the atmosphere through the application as solvent for the production of glue, resins, cellulose, rubber, paraffin wax and lacquer (Ware, 1988).

Tropospheric MEK gas-phase concentration was found to be in the range of $0.02 - 15$ ppbv, depending on the region (Grosjean et al., 2002; Riemer et al., 1998; Singh et al., 2004; Snider and Dawson, 1985; Goldan et al., 1995; Grosjean et al., 1983; Grosjean, 1982; Müller et al., 2005; Feng et al., 2004). Singh et al. (2004) measured a concentration in a remote region of 0.02 ppbv, whereas Grosjean et al. (1983) observed a MEK concentration of 11.3 ppbv in Los Angeles. Brown et al. (1994) concluded that MEK is one of the major volatile organic compounds (VOCs) in indoor air.

In addition to the gas-phase measurements, the concentrations measured in bulk water samples collected at an open station near the Bahamas reached a concentration of $< 0.5$ nmol $L^{-1}$ (Zhou and Mopper, 1997). Furthermore, an enrichment of MEK in the surface micro layer was found with concentrations up to 2.28 nmol $L^{-1}$ (Zhou and Mopper, 1997). MEK was also investigated in ice, fog, and rain samples (Grosjean and Wright, 1983). It was not found in fog but there were traces in rain water. In cloud water, a concentration of up to 650 nmol $L^{-1}$ was measured. This is supported by van Pinxteren et al. (2005), who measured a concentration of 70 to 300 nmol $L^{-1}$ in cloud water. These studies concluded that the liquid-phase fraction of MEK is higher than the expected fraction calculated according to the Henry constant.

The Henry constants at a temperature of 25 °C were found to vary between 7.7 and 21 M atm$^{-1}$ in numerous studies (Buttery et al., 1969; Snider and Dawson, 1985; Ashworth et al., 1988; Zhou and Mopper, 1990; Morillon et al., 1999; Karl et al., 2002). However, Schütze and Herrmann (2004) estimated the Henry constant to be between 23 and 50 M atm$^{-1}$, which is higher than the previous measured values found in the literature. This higher Henry constant supports the conclusion from van Pinxteren et al. (2005) and tends to support the investigation of MEK in the liquid phase as aqSOA precursor compound. AqSOA is formed through the oxidation of organic compounds in the aqueous particle phase and is often related to missing SOA sources. These missing sources are most likely responsible for the huge discrepancies between measured and calculated SOA burden. As model results usually underestimate the SOA burden (Kanakidou et al., 2005; Goldstein and Galbally, 2007), missing SOA sources have to be considered in such models to close this gap (Ervens et al., 2011; Herrmann et al., 1999; Herrmann et al., 2015).

In the present study, the reaction of MEK with OH radicals in water was investigated. Based on the experimentally obtained data, a reaction mechanism was developed to explain methylglyoxal formation. The

57 mechanism was included in a COPASI (Complex Pathway Simulator) model and evaluated by comparing the
58 experimentally obtained data and the model results.

59 **2. Experimental**

60 2.1 Chemicals and standards

61 Cyclohexanone-2,2,6,6-d4 (98%), hydrochloric acid, and catalase from bovine liver (40000-60000 units mg$^{-1}$

62 protein) were obtained from Sigma-Aldrich (Hamburg, Germany). $O$-(2,3,4,5,6-

63 pentafluorobenzyl)hydroxylamine hydrochloride ($\geq$99%), 2,3-butanedione (99%), hydroxyacetone (90%), and

64 methylglyoxal (40% in water) were purchased from Fluka (Hamburg, Germany). Dichloromethane (Chromasolv

65 99.8%) and methyl ethyl ketone (99.7%) were obtained from Riedel-de Haen (Seelze, Germany), and hydrogen

66 peroxide (30% Suprapur®) was obtained from Merck KGaA (Darmstadt, Germany). Ultrapure water was used to

67 prepare the reaction solutions for the bulk reactor experiments and the stock solutions of the authentic standard

68 compounds (Milli-Q gradient A 10, 18.2 M$\Omega$ cm$^{-1}$, 3 ppb TOC, Millipore, USA).

69 2.2 Bulk reactor experiments

70 The aqueous-phase oxidation of MEK was conducted in a 300 mL batch reactor using the photolysis of hydrogen

71 peroxide (H$_2$O$_2$) as an OH radical source (Set 1). The experiments were conducted at a temperature of 298 K. For

72 the experiments, 0.1 mmol L$^{-1}$ of the precursor compound was mixed with 2 mmol L$^{-1}$ of H$_2$O$_2$. The solution was

73 then irradiated at $\lambda$ = 254 nm for 4 hours to continuously generate OH radicals (500 W xenon-mercury lamp,

74 Andover Corporation Optical bandpass filter: L.O.T.- Oriel GmbH & Co. KG, Darmstadt, Germany). To obtain

75 time-resolved data, samples were taken once per hour (0 – 4 hours; number of repetitions n = 3) or in steps of

76 15 minutes (n = 1) and analyzed after derivatization using GC/MS. To avoid further reactions of the organics

77 present in the sample with remaining H$_2$O$_2$, 100 $\mu$L of catalase (4 mg mL$^{-1}$ in water) were added to each sample.

78 Furthermore, a set of blank experiments was conducted to exclude that (a) MEK reacts with H$_2$O$_2$ (Set 2),

79 (b) identified oxidation products originate from photolysis (Set 3), (c) the photolysis of contaminants in the H$_2$O$_2$

80 solution results in the formation of organics (Set 4), and (d) oxidation of 2,3-butanedione or hydroxyacetone also

81 forms methylglyoxal (Set 5/6). To determine the photolysis rate constants of 2,3-butanedione, methylglyoxal, and

82 hydroxyacetone, the photolysis of these products was investigated as well with the setup used (Set 7). A complete

83 overview of the experiments conducted is given in Table 1.

84 2.3 Sample preparation

85 Two types of samples were taken over a period of 4 hours. For the first type of samples, 60 $\mu$L of the reaction

86 mixture were diluted with 2940 $\mu$L of water to avoid saturation of the GC/MS detector during the quantification

87 of MEK, 2,3-butanedione or hydroxyacetone. For the second type of samples, 3 mL of the reaction mixture were

88 taken and injected without any dilution to enable the identification and quantification of the formed carbonyl

89 compounds.

90 Samples of all sets were derivatized with 300 $\mu$L of $o$-(2,3,4,5,6-pentafluorobenzyl)hydroxylamine

91 hydrochloride (PFBHA, 5 mg mL$^{-1}$) at room temperature (Rodigast et al., 2015). Cyclohexanone-2,2,6,6-d4 was

92 used as an internal standard (150 $\mu$L, 100 $\mu$mol L$^{-1}$), and after 24 hours, a pH value of 1 was adjusted by adding

93 hydrochloric acid (37%) to the reaction mixture. The target compounds were extracted for 30 minutes with 250 $\mu$L

94 of dichloromethane using an orbital shaker (1500 rpm, revolutions per minutes). Finally, 1 $\mu$L of the organic phase

95    was used for GC/MS analysis. A 5-point calibration was performed for each chromatographic run using a series

96    of the standard solutions (MEK, methylglyoxal, 2,3-butanedione, and hydroxyacetone) with concentrations

97    ranging from 1 to 50 μmol L$^{-1}$.

98    2.4 Instrumentation

99    Derivatized carbonyl compounds were analyzed using a GC System (6890 Series Agilent Technologies, Frankfurt,

100    Germany) coupled with an electron ionization quadrupole mass spectrometer in splitless mode at a temperature

101    of 250 °C (Agilent 5973 Network mass selective detector, Frankfurt, Germany). They were separated with an HP-

102    5MS UI column (Agilent J & W GC columns, 30 m × 0.25 mm × 0.25 μm) using the following temperature

103    program: 50 °C isothermal for 2 minutes and elevated to 230 °C with 10 °C minute$^{-1}$. The temperature of 230 °C

104    was held for 1 minute, and the temperature gradient ended with 320 °C, which was held constant for 10 minutes.

105    2.4 Instrumentation

106    Derivatised carbonyl compounds were analysed using a GC System (6890 Series Agilent Technologies, Frankfurt,

107    Germany) coupled with an electron ionization quadrupole mass spectrometer (Agilent 5973 Network mass

108    selective detector, Frankfurt, Germany) in the splitless mode at a temperature of 250 °C. They were separated

109    with a HP-5MS UI column (Agilent J & W GC columns, 30 m × 0.25 mm × 0.25 μm) using the following

110    temperature program: 50 °C isothermal for 2 minutes and elevated to 230 °C with 10 °C minute$^{-1}$. The temperature

111    of 230 °C was held for 1 minute and the temperature gradient ended with 320 °C which was held constant for

112    10 minutes.

113    **3. Results**

114    **3.1 Experimental results from bulk reactor**

115    MEK was oxidized with OH radicals, and the decay of MEK was monitored by GC/MS. Fig. 1A shows the

116    consumption of the precursor compound MEK. As can be seen, MEK was almost consumed after 180 minutes of

117    reaction time. From the analysis of the collected samples, 2,3-butanedione, hydroxyacetone, and methylglyoxal

118    were observed as the most dominating oxidation products. The formation of methylglyoxal from the oxidation of

119    MEK was unexpected as it has not been reported in the literature before. Due to the relevance of methylglyoxal

120    for aqSOA formation, its formation was comprehensively characterized in the present study.

121    Nevertheless, in Fig. 1B, 2,3-butanedione was found as the main oxidation product of MEK reaching a

122    maximum yield of ≈ 29.5 ± 6.0% after 60 minutes. The small variations of the molar yields over the course of the

123    experiment might result from slight temperature changes during the experiment despite the reactor temperature

124    being controlled. However, the curve shape shows that the concentration of 2,3-butanedione starts to decrease

125    after 60 minutes, indicating further reactions of 2,3-butanedione. This decrease results in a molar yield of

126    18.9 ± 3.9% at the end of the experiment (240 minutes).

127    A similar trend was observed for hydroxyacetone and methylglyoxal, as the concentration of

128    methylglyoxal was the highest after 15 minutes (≈ 9.5%) and started to decrease afterwards. In comparison,

129    hydroxyacetone reached the highest concentration after 60 minutes with a molar yield of 3.0 ± 2.6%. The standard

130    deviation of the determined molar yields of hydroxyacetone was high, and therefore, only after reaction times of

131    60 and 120 minutes could a molar yield of hydroxyacetone be determined.

132  Methylglyoxal and hydroxyacetone were completely consumed at the end of the experiment. The strong
133  decrease of the concentrations of the detected carbonyl compounds might result from the reaction with OH radicals
134  and/or from photolysis. Both mechanisms are most likely, as it has been demonstrated that the detected carbonyl
135  compounds react quickly with OH radicals (Lilie et al., 1968; Gligorovski and Herrmann, 2004; Doussin and
136  Monod, 2013; Monod et al., 2005; Ervens et al., 2003; Herrmann et al., 2005; Tan et al., 2010; Stefan and Bolton,
137  1999) and they are prone to photolysis (Faust et al., 1997; Tan et al., 2010). The photolysis rate constants of the
138  detected carbonyl compounds were determined in the present study because of the dependency on the setup used
139  (Set 7; see supplement S2 for more details). Methylglyoxal and hydroxyacetone showed higher photolysis rate
140  constants of $k_p = 3 \times 10^{-5}$ s$^{-1}$ and $k_p = 2 \times 10^{-5}$ s$^{-1}$ in comparison to 2,3-butanedione ($k_p = 9 \times 10^{-6}$ s$^{-1}$). This
141  indicates a faster decomposition compared to 2,3-butanedione of methylglyoxal and hydroxyacetone, which
142  showed a complete consumption at the end of the experiment (Fig. 1). 2,3-Butanedione was not completely
143  consumed during the reaction time of 4 hours, which might be a result of the lower photolysis rate constants.
144  Furthermore, during the photolysis of 2,3-butanedione and hydroxyacetone, methylglyoxal was found with molar
145  yields of $\approx 17\%$ and $\approx 19\%$, respectively (see Fig. S2, supplement S2). Due to the low molar yield of
146  hydroxyacetone during the oxidation of MEK ($\approx 3\%$) and the slow photolysis rate constant of 2,3-butanedione,
147  these processes are of minor importance for the methylglyoxal yield.

148  For 2,3-butanedione, a huge discrepancy of the rate constants for the OH radical oxidation can be found
149  between the different literature studies. They vary by one order of magnitude in a range of $k = 1.4 \times 10^8$ M$^{-1}$ s$^{-1}$
150  (Gligorovski and Herrmann, 2004) up to $k = 1.86 \times 10^9$ M$^{-1}$ s$^{-1}$ (Doussin and Monod, 2013). Rate constants were
151  determined between $k = 5.3 \times 10^8$ M$^{-1}$ s$^{-1}$ and $k = 1.1 \times 10^9$ M$^{-1}$ s$^{-1}$ for methylglyoxal (Monod et al., 2005; Ervens
152  et al., 2003; Herrmann et al., 2005; Tan et al., 2010) and between $k = 0.8 \times 10^9$ M$^{-1}$ s$^{-1}$ and $k = 1.2 \times 10^9$ M$^{-1}$ s$^{-1}$
153  for hydroxyacetone (Stefan and Bolton, 1999; Herrmann et al., 2005). In consideration of the similar rate constant
154  for 2,3-butanedione determined by Lilie et al. (1968) ($k = 1.8 \times 10^8$ M$^{-1}$ s$^{-1}$) and Gligorovski and Herrmann (2004)
155  ($k = 1.4 \times 10^8$ M$^{-1}$ s$^{-1}$), 2,3-butanedione revealed a slower OH radical reaction than methylglyoxal and
156  hydroxyacetone. This is in good agreement with the experimental results obtained in the present study.

157  Since 2,3-butanedione is the main oxidation product, it was necessary to investigate the contribution of
158  2,3-butanedione to the product distribution, especially for the formation of methylglyoxal. In the oxidation of 2,3-
159  butanedione (Set 5), no methylglyoxal was detected in the GC/MS chromatogram over a reaction period of
160  240 min (Fig. 2). Consequently, a contribution of 2,3-butanedione to the methylglyoxal formation could be
161  excluded.

162  Despite the low molar yield of hydroxyacetone during MEK oxidation, the oxidation of hydroxyacetone
163  was investigated for methylglyoxal formation as well (Herrmann et al., 2005; Schaefer et al., 2012; Set 6). During
164  the oxidation, a molar yield of 100% was found after a reaction time of 60 minutes (see supplement S3, Fig. S3).
165  After 60 minutes of reaction time, the molar yield of methylglyoxal decreases through further reactions, as was
166  observed during MEK oxidation. However, due to the low molar yield of hydroxyacetone (3.0%), the oxidation
167  has only minor importance for the observed molar yield of methylglyoxal.

168  To ensure methylglyoxal was only formed during the oxidation of MEK, an experiment was conducted
169  to investigate the non-radical reaction of MEK with $H_2O_2$ in the dark (Set 2). During this experiment, no
170  decomposition of MEK was observed, excluding the non-radical reaction of MEK with $H_2O_2$ as a source of
171  methylglyoxal. Furthermore, the photolysis of MEK has to be considered as a source for methylglyoxal. Hence,

172    the photolysis of MEK was studied at λ = 254 nm (Set 3). As can be seen in Fig. 3, the photolysis of MEK leads
173    to the formation of 2,3-butanedione with a molar yield of ≈ 2.2% indicating that the photolysis of MEK is an
174    additional source. No further carbonyl compounds were detected from the photolysis of MEK, and thus, the
175    photolysis of MEK can be excluded as a methylglyoxal source. The blank experiment (Set 4) indicated the absence
176    of methylglyoxal as well.

177         In summary, the oxidation of MEK constitutes a source for methylglyoxal, and due to the high
178    concentration of MEK in cloud water (70 – 650 nmol L$^{-1}$; Grosjean and Wright, 1983; van Pinxteren et al., 2005),
179    this source is of atmospheric relevance. Due to the molar yields of 9.5% for methylglyoxal, 29.5% for 2,3-
180    butanedione, and 3.0% for hydroxyacetone, ≈ 42% of the oxidation products of MEK could be elucidated in the
181    present study with only these carbonyl compounds (Table 2). This highlights the importance of carbonyl
182    compounds for the aqueous phase chemistry. Based on the experimental findings, a reaction mechanism was
183    developed to describe the formation of methylglyoxal (Fig. 4).

184    **3.2 Oxidation mechanism and model description**
185    According to the structure of MEK, the OH radical attack can proceed at three different positions (Fig. 4; H-atoms
186    at carbons 1, 3, and 4). For the present study, only the attack at carbons 3 and 4 is considered because these
187    processes lead to the formation of the observed products (Fig. 4). Note that the abstraction of a hydrogen atom at
188    carbon 3 leads to a secondary alkyl radical (A), whereas at the terminal carbon, a primary alkyl radical is formed
189    (B). The branching ratios for the formation of the primary and secondary alkyl radicals will be discussed in detail
190    in the next section (Sect. 3.2.1).
191    The primary and secondary alkyl radicals react rapidly with oxygen to form alkylperoxy radicals. The alkylperoxy
192    radical recombines to a tetroxide and reacts further in three different ways, including the formation of an carbonyl
193    compound and an alcohol (i), the formation of two carbonyl compounds and H$_2$O$_2$ (ii), and the decomposition into
194    an alkoxy radical (iii) (von Sonntag and Schuchmann, 1991). The decomposition of the tetroxide into a peroxide
195    and oxygen was not considered further due to the minor importance of this process (von Sonntag and Schuchmann,
196    1997). The secondary and primary alkylperoxy radicals can react with HO$_2$, forming organic hydroperoxides. The
197    organic peroxides react with OH radicals or photolyze, resulting in the formation of an alkoxy radical or tetroxide
198    that can react further, as described before through pathways i–iii. The described mechanism was included in a
199    COPASI model to examine the developed oxidation mechanism, the decomposition of the precursor compound,
200    and the formation of the observed products. Table 3 shows the considered reactions, the rate constants, and their
201    references. Only the reactions leading to the formation of the products identified are discussed in detail.
202    Surprisingly, the products 3-oxobutanal and hydroxybutanone were not observed during the experiments. Since
203    3-oxobutanal contains two carbonyl groups, two derivatives can be formed, including one (mass to charge ratio
204    $m/z$ 281; M$^{•+}$) or two ($m/z$ 476; M$^{•+}$) derivatized groups. Hydroxybutanone has one carbonyl group with a
205    derivatized $m/z$ 283 (M$^{•+}$). As can be seen in Fig. 5, $m/z$ 283 was not found in the extracted ion chromatogram
206    (EIC). Furthermore, $m/z$ 281 and 476 can be detected in the EIC of the bulk reactor samples, but they can also be
207    found in the EIC of the authentic standard compounds. The sample of the authentic standard compounds does not
208    contain hydroxybutanone and 3-oxobutanal. According to the comparison of the EIC of the bulk reactor samples
209    and the authentic standard, it can be assumed that $m/z$ 281 and 476 are fragments of the internal standard and 2,3-
210    butandione. No additional signals in the EIC of the samples were detected at $m/z$ 281, 283, and 476, and thus, 3-

oxobutanal and hydroxybutanone are not formed during the experiment. Hence, their formation pathways were excluded from the model.

### 3.2.1 HO$_x$ chemistry and OH radical attack

The relevant reactions for HO$_x$ chemistry according to R1-R6 are included in the mechanism. OH radicals were formed through the photolysis of H$_2$O$_2$ at $\lambda = 254$ nm with measured photolysis rate constants of $k_p = 7.6 \times 10^{-6}$ s$^{-1}$ (R1, see supplement S1). The formed OH radicals react further with MEK in a first oxidation step, leading to the formation of a primary (R7) and secondary alkyl radical (R8). The rate constants were postulated by Herrmann et al. (2005) to be $k = 1.17 \times 10^8$ M$^{-1}$ s$^{-1}$ and $k = 1.3 \times 10^9$ M$^{-1}$ s$^{-1}$ for the formation of the primary and secondary alkyl radicals, respectively. This is in good agreement with the model study by Sebbar et al., who postulated that the H-atom abstraction most likely proceeds at the secondary carbon of MEK (Sebbar et al., 2014; Sebbar et al., 2011) due to the lower C-H bond dissociation energy ($\approx 377$ kJ mol$^{-1}$, C4) in comparison to the primary carbon atom ($\approx 423$ kJ mol$^{-1}$, C3). In the present study, a rate constant $k = 1.5 \times 10^9$ M$^{-1}$ s$^{-1}$ (Gligorovski and Herrmann, 2004) was used, and the branching ratio was varied from 60/40 to 10/90 for the primary/secondary H-atom abstraction.

The results are shown in Fig. 6 and discussed based on the molar yields of the products. As can be seen for 2,3-butanedione (Fig. 6A), a branching ratio of 60% for the primary H-atom abstraction and 40% for the secondary H-atom abstraction leads to lower molar yields, whereas the molar yields start to increase with an increasing fraction of secondary H-atom abstraction. According to the mechanism (Fig. 4), 2,3-butanedione is only formed via secondary H-atom abstraction, and thus, it is feasible to reach higher molar yields with a higher fraction of secondary H-atom abstraction. However, with an increasing secondary H-atom abstraction, the experimentally determined concentration was increasingly overestimated, especially at the beginning of the experiment. After 60 minutes of reaction time, the highest experimentally determined molar yield ($29.5 \pm 6.0\%$) was overestimated by a factor of $\approx 2$ with a ratio of 10/90 for primary/secondary H-atom abstraction (molar yield $\approx 49.9\%$), whereas a ratio of 60/40 resulted in reasonably good agreement (molar yield $\approx 23.7\%$). Based on this, a branching ratio of 60/40 for primary/secondary H-atom abstraction was used in the present model.

In contrast, methylglyoxal molar yields were increasingly underestimated with an increasing fraction of secondary H-atom abstraction (Fig. 6B). Thus, after 15 minutes of reaction time, the experimental molar yield ($\approx 9.5\%$) was underestimated by a factor of $\approx 5$ with a higher fraction of the secondary H-atom abstraction (molar yield $\approx 2\%$). In comparison with a ratio of 60/40 for primary/secondary H-atom abstraction, a molar yield of $\approx 11.4\%$ was observed, which is in good agreement with the experiment. Overall, the branching ratio of 60/40 (primary/secondary H-atom abstraction) resulted in reasonable agreement for 2,3-butanedione and in an excellent conformity to the methylglyoxal molar yields. This shows the importance of the primary H-atom abstraction as the main decomposition pathway of MEK and thus for methylglyoxal formation.

The primary and secondary alkyl radicals react further with oxygen (R9/R21) with a rate constant of $k = 3.1 \times 10^9$ M$^{-1}$ s$^{-1}$ (Zegota et al., 1986; Glowa et al., 2000), which was reported for the formation of acetonylperoxy radicals. The rate constants of the acetonylperoxy radical were used for the formation of the primary alkylperoxy radical (R9) and further reactions of the alkylperoxy radical because of their structural similarity. They were also applied by Glowa et al. (2000) for the formation of the secondary alkylperoxy radical of MEK. Further reactions of the primary and secondary alkylperoxy radicals resulting in different oxidation products will be discussed in detail in the following section (Sect. 3.2.2 and 3.2.3).

*3.2.2 Oxidation of MEK leading to the formation of methylglyoxal and hydroxyacetone*

Only the formation of the alkoxy radical (iii; R10) leads to the formation of methylglyoxal. The alkoxy radical further reacts rapidly with oxygen into an acetonylperoxy radical under elimination of formaldehyde. The acetonylperoxy radicals can recombine again to form a tetroxide (Schaefer et al., 2012). The latter is able to decompose through pathways i–iii, which are illustrated in R11–R13. Consequently, the decomposition of the tetroxide can explain the formation of hydroxyacetone and methylglyoxal (R11; $k = 2 \times 10^8$ $M^{-1}$ $s^{-1}$; Zegota et al., 1986), methylglyoxal (R12; $k = 4 \times 10^7$ $M^{-1}$ $s^{-1}$; Zegota et al., 1986), and methylglyoxal and hydrogen peroxide (R13; $k = 4 \times 10^8$ $M^{-1}$ $s^{-1}$; Zegota et al., 1986; Schaefer et al., 2012).

In addition to the discussed pathway, the primary alkylperoxy radical has the opportunity to react with $HO_2$ instead of the recombination, forming an organic hydroperoxide (R14). The rate constant was reported by von Sonntag and Schuchmann (1991) to be from $10^7$ $M^{-1}$ $s^{-1}$ up to $10^9$ $M^{-1}$ $s^{-1}$. For the primary alkylperoxy radical, $k = 1 \times 10^7$ $M^{-1}$ $s^{-1}$ was used as it led to the best agreement of the experimental data and the model results. The formed peroxide can react with OH radicals (R15) or photolyze (R16). The same rate constant ($k = 2.7 \times 10^7$ $M^{-1}$ $s^{-1}$) as that for the OH radical oxidation of $H_2O_2$ was used for R15 due to a lack of literature data. According to the assumption by Monod et al. (2007), the rate constant for the photolysis of the formed peroxide (R16) was defined to be 1/10 of the photolysis rate constants of hydrogen peroxide. Thus, a photolysis rate constant of $k_p = 7.6 \times 10^{-7}$ $s^{-1}$ was included in the model. This was used as a first approximation due to a lack of literature data for the formed hydroperoxides. The photolysis of the organic peroxide leads to the formation of formaldehyde, OH radicals, and an acetonyl radical, which reacts further with oxygen (R17) to form an acetonylperoxy radical ($k = 3.1 \times 10^9$ $M^{-1}$ $s^{-1}$; Zegota et al., 1986; R19) and subsequently methylglyoxal (R18 – 20).

*3.2.3 Oxidation of MEK leading to the formation of methylglyoxal and 2,3-butanedione*

As described for the primary alkylperoxy radical, the secondary alkylperoxy radical recombines and forms a tetroxide. This reacts to form either (i) 2,3-butanedione and acetoin (R22) or (ii) 2,3-butanedione and hydrogen peroxide (R23) and is considered with rate constants of $k = 2.5 \times 10^8$ $M^{-1}$ $s^{-1}$ and $k = 4.5 \times 10^8$ $M^{-1}$ $s^{-1}$ (Glowa et al., 2000). The tetroxide can decompose into an alkoxy radical as well (iii) and react further to form 2,3-butanedione, methylglyoxal, a methyl radical, and $HO_2$ (R24; $k = 5 \times 10^7$ $M^{-1}$ $s^{-1}$; Glowa et al., 2000). The rate constants postulated by Glowa et al. (2000) are derived from the branching ratios determined by Zegota et al. (1986) for acetone. Glowa et al. (2000) simulated the concentration profiles of MEK and the corresponding products and postulated the rate coefficient used in the present model study. The secondary alkylperoxy radical also has the opportunity to react with $HO_2$ to form an organic peroxide (R25), which photolyzes (R26; $k = 7.6 \times 10^{-7}$ $s^{-1}$) or reacts further with OH radicals (R28; $k = 2.7 \times 10^7$ $M^{-1}$ $s^{-1}$). Through the photolysis, an alkoxy radical was formed that leads to methylglyoxal, 2,3-butanedione, a methyl group, and $HO_2$ radicals (R27; $k = 4 \times 10^7$ $M^{-1}$ $s^{-1}$).

*3.2.4 Further reactions and photolysis of formed oxidation products and MEK*

The products 2,3-butanedione, methylglyoxal, and hydroxyacetone positively identified by GC/MS analysis might also react further, forming a variety of oxidation products. The rate constant of methylglyoxal with OH radicals is given in the range of $k = 5.3 \times 10^8$ $M^{-1}$ $s^{-1}$ to $k = 1.1 \times 10^9$ $M^{-1}$ $s^{-1}$ (Monod et al., 2005; Ervens et al., 2003; Herrmann et al., 2005; Tan et al., 2010), whereas a rate constant of $k = 5.3 \times 10^8$ $M^{-1}$ $s^{-1}$ (R29; Monod et al., 2005)

leads to the best agreement between the experimental data and the model results. In comparison, the rate constants determined by Ervens et al. (2003), Herrmann et al. (2005), and Tan et al. (2010) resulted in an underestimation of the molar yield. Methylglyoxal also has the opportunity to photolyze. The photolysis is included with $k_p = 3 \times 10^{-5}$ s$^{-1}$ (R30) in the present model.

2,3-Butanedione is also prone to OH radical oxidation and photolysis. As discussed, a huge discrepancy exists in the rate constants for the reaction of OH radicals with 2,3-butanedione (Lilie et al., 1968; Doussin and Monod 2013; Gligorovski and Herrmann, 2004). In the present study, the value of $k = 1.4 \times 10^8$ M$^{-1}$ s$^{-1}$ (R31) determined by Gligorovski and Herrmann (2004) was used. The higher rate constants reported by Lilie et al. (1968) and Doussin and Monod (2013) resulted in consumption that was too fast. The photolysis was included with a rate constant of $k_p = 9 \times 10^{-6}$ s$^{-1}$ in the COPASI model (R32). It should be mentioned that methylglyoxal was formed during the photolysis of 2,3-butanedione. However, the photolysis was too small to contribute significantly to methylglyoxal formation. For more details, see supplement S2.

The oxidation of hydroxyacetone with OH radicals was also considered in the model study with a rate constant of $k = 8 \times 10^8$ M$^{-1}$ s$^{-1}$ (R33; Stefan and Bolton, 1999). During the experiment, methylglyoxal was formed with 100% molar yield. Thus, the reaction of hydroxyacetone to methylglyoxal was included in the model study. The photolysis of hydroxyacetone was measured with a rate of $k_p = 2 \times 10^{-5}$ s$^{-1}$, leading to methylglyoxal with a molar yield of $\approx 19\%$ (R34). The photolysis rate constant of MEK was measured as $k_p = 5 \times 10^{-5}$ s$^{-1}$ (see supplement S2, Fig. S1). During the experiment, 2,3-butanedione was found with a molar yield of 2.2%. Thus, the reaction of MEK leading to 2,3-butanedione was included in the model study (R35).

### 3.3 Model results and comparison with the experimental dataset

The described reactions are included in a model, and the decomposition of MEK and molar yields of formed products were compared to the experimentally obtained data (Fig. 7). The model was not validated with the time course of hydroxyacetone due to the high standard deviation of the experimental results. The comparison of the model study and the experiment showed very good agreement for the consumption of MEK (Fig. 7A). There is also good agreement for the formation of methylglyoxal and limited agreement for the molar yields of 2,3-butanedione. The initial high molar yield of 2,3-butanedione is reflected well (Fig. 7B). Thus, after 60 minutes of reaction time, molar yields of 23.7% in the model study and 29.5 ± 6.0% in the experiment were reached. Under consideration of the standard deviation, this is in good agreement with the COPASI model.

The determined molar yields up to a reaction time of 120 minutes showed very good conformity with the experiment (18.2% and 22.1 ± 9.0%). The temporal behavior shows that the determined molar yield in the model study is somewhat lower towards the end of the experiment. Hence, it is possible that there are other reaction pathways that lead to higher molar yields of 2,3-butanedione at the end of the experiment, which are not considered in the model study as of now. Good agreement between the model results and experiment was observed for methylglyoxal (Fig. 7C). The curve shapes are very similar, and hence, fast formation and decomposition of methylglyoxal were found in the model study and in the experiment. After 15 minutes of reaction time, a molar yield of 9.5% was found in the experiment. In comparison, the model study resulted in a molar yield of 11.4%, which is in good agreement with the experiment and validates the COPASI model.

**4. Atmospheric relevance**

The sources of methylglyoxal in the aqueous phase are thus-far not fully elucidated. Methylglyoxal can originate in the atmospheric aqueous phase through i) uptake from the gas phase, and/or ii) formation in the aqueous phase. The importance of the uptake from the gas into the aqueous phase is discussed in the literature but large discrepancies can be found. Kroll et al. (2005) investigated the uptake of methylglyoxal on inorganic seed particles under varying relative humidity. It was found that the uptake was not relevant for methylglyoxal even under high relative humidity. Contrary, Zhao et al. (2006) measured an uptake coefficient of $\gamma = 7.6 \times 10^{-3}$ on acidic solution. They found an irreversible uptake, which decreases with increasing acidity. Fu et al. (2008, 2009) determined an uptake coefficient on aqueous particles and cloud droplets $\gamma = 2.9 \times 10^{-3}$, which is in good agreement with the uptake coefficient measured by Zhao et al. (2006). Lin et al. (2014) modelled an uptake coefficient for several case studies with different multiphase process mechanisms. The uptake coefficient in deliquescent particles was determined to be $\gamma = 1.47 - 2.92 \times 10^{-5}$. Overall, $\gamma$ was two orders of magnitude lower compared to the values determined by Zhao et al. (2006) and Fu et al. (2008, 2009) showing the discrepancies between the different studies available in literature.

The in-situ formation of methylglyoxal in the aqueous phase could be an important source as well (Blando and Turpin, 2000; Sempere and Kawamura 1994). Within the present study, MEK was found as a new precursor compound for methylglyoxal in the aqueous phase yielding methylglyoxal with a molar yield of 9.5%. Although the Henry constant of MEK (up to $K_H = 50$ M atm$^{-1}$, Schütze and Herrmann, 2004) is lower compared to methylglyoxal ($K_H = 3.7 \times 10^3$ M atm$^{-1}$, Betterton and Hoffmann, 1988), van Pinxteren et al. (2005) found higher concentrations in cloud water as it was expected. Thus, the phase transfer of MEK from the gas in the aqueous phase could be more important as currently derived from the available Henry constants. Besides the phase transfer, the in-situ formation of MEK in aqueous phase formation might also represents an important source.

As, the oxidation of MEK yielding methylglyoxal has not been studied much before, it should be considered as a formation process of methylglyoxal.

**5. Summary**

In the present study, MEK was identified as a new source for methylglyoxal in the aqueous phase. It was demonstrated that methylglyoxal originates directly from MEK oxidation and not from side reactions such as photolysis or non-radical reactions. A molar yield of $\approx 9.5\%$ was determined during the oxidation. Based on the experimental results, a reaction mechanism could be developed. The calculations with a COPASI model supported the experimental results and confirm MEK as a precursor compound for methylglyoxal in aqueous medium.

Further carbonyl compounds could be identified and quantified. 2,3-Butanedione was found as the main oxidation product (molar yield $\approx 29.5\%$) and was formed during the photolysis of MEK as well. As a further oxidation product, hydroxyacetone was identified and was formed with a molar yield of $\approx 3.0\%$ during the oxidation of MEK.

The oxidation mechanism of MEK in aqueous solution was elucidated, and MEK was demonstrated to be as a precursor compound for methylglyoxal in the aqueous phase. Regarding the important role of methylglyoxal for the aqSOA formation, MEK has to be considered for aqSOA as well, which could be a next step in reducing the underestimation of the SOA burden by model studies.

369 **References**

370 Akagi, S. K., Yokelson, R. J., Wiedinmyer, C., Alvarado, M. J., Reid, J. S., Karl, T., Crounse, J. D., and Wennberg,
371      P. O.: Emission factors for open and domestic biomass burning for use in atmospheric models, Atmos. Chem.
372      Phys., 11, 4039-4072, 10.5194/acp-11-4039-2011, 2011.

373 Andreae, M. O., and Merlet, P.: Emission of trace gases and aerosols from biomass burning, Glob. Biogeochem.
374      Cycle, 15, 955-966, 10.1029/2000gb001382, 2001.

375 Ashworth, R. A., Howe, G. B., Mullins, M. E., and Rogers, T. N.: Air water partitioning coefficients of organics
376      in dilute aqueous-solutions, J. Hazard. Mater., 18, 25-36, 10.1016/0304-3894(88)85057-x, 1988.

377 Atkinson, R.: Gas-phase tropospheric chemistry of volatile organic compounds .1. Alkanes and alkenes, J. Phys.
378      Chem. Ref. Data, 26, 215-290, 1997.

379 Blando, J. D., and Turpin B. J.: Secondary organic aerosol formation in cloud and fog droplets: a literature
380      evaluation of plausibility, Atmos. Environ., 34, 1623-1632, 2000.

381 Brilli, F., Gioli, B., Ciccioli, P., Zona, D., Loreto, F., Janssens, I. A., and Ceulemans, R.: Proton Transfer Reaction
382      Time-of-Flight Mass Spectrometric (PTR-TOF-MS) determination of volatile organic compounds (VOCs)
383      emitted from a biomass fire developed under stable nocturnal conditions, Atmospheric Environment, 97, 54-
384      67, 10.1016/j.atmosenv.2014.08.007, 2014.

385 Brown, S. K., Sim, M. R., Abramson, M. J., and Gray, C. N.: Concentrations of volatile organic-compounds in
386      indoor air - a review, Indoor Air-Int. J. Indoor Air Qual. Clim., 4, 123-134, 10.1111/j.1600-0668.1994.t01-2-
387      00007.x, 1994.

388 Buttery, R. G., Ling, L. C., and Guadagni, D. G.: Food volatiles - volatilities of aldehydes ketones and esters in
389      dilute water solution, J. Agric. Food Chem., 17, 385-&, 10.1021/jf60162a025, 1969.

390 Buyske, D. A., Owen, L. H., Wilder, P., and Hobbs, M. E.: Chromatography of the 2,4-dinitrophenylhydrazones
391      of some aldehydes and ketones in tobacco smoke, Anal. Chem., 28, 910-913, 10.1021/ac60113a040, 1956.

392 Carlier, P., Hannachi, H., and Mouvier, G.: The chemistry of carbonyl-compounds in the atmosphere - a review,
393      Atmospheric Environment, 20, 2079-2099, 10.1016/0004-6981(86)90304-5, 1986.

394 Christensen, H., Sehested, K., and Corfitzen, H.: Reactions of hydroxyl radicals with hydrogen-peroxide at
395      ambient and elevated-temperatures, J. Phys. Chem., 86, 1588-1590, 10.1021/j100206a023, 1982.

396 Christensen, H., and Sehested, K.: $HO_2$ and $O_2-$ radicals at elevated-temperatures, J. Phys. Chem., 92, 3007-3011,
397      10.1021/j100321a060, 1988.

398 Ciccioli, P., Brancaleoni, E., Frattoni, M., Cecinato, A., and Brachetti, A.: Ubiquitous occurrence of semivolatile
399      carbonyl-compounds in tropospheric samples and their possible sources, Atmospheric Environment Part a-
400      General Topics, 27, 1891-1901, 10.1016/0960-1686(93)90294-9, 1993.

401 de Gouw, J. A., Howard, C. J., Custer, T. G., and Fall, R.: Emissions of volatile organic compounds from cut
402      grasses and clover are enhanced during the drying process, Geophysical Research Letters, 26, 811-814, 1999.

403 Doussin, J. F., and Monod, A.: Structure-activity relationship for the estimation of OH-oxidation rate constants
404      of carbonyl compounds in the aqueous phase, Atmos. Chem. Phys., 13, 11625-11641, 10.5194/acp-13-11625-
405      2013, 2013.

406 Elliot, A. J., and Buxton, G. V.: Temperature-dependence of the reactions OH + $O_2^-$ and OH + $HO_2$ in water up
407      to 200 °C, J. Chem. Soc.-Faraday Trans., 88, 2465-2470, 10.1039/ft9928802465, 1992.

408 Ervens, B., Gligorovski, S., and Herrmann, H.: Temperature-dependent rate constants for hydroxyl radical
409      reactions with organic compounds in aqueous solutions, Phys. Chem. Chem. Phys., 5, 1811-1824,
410      10.1039/b300072a, 2003.

411 Ervens, B., Turpin, B. J., and Weber, R. J.: Secondary organic aerosol formation in cloud droplets and aqueous
412      particles (aqSOA): a review of laboratory, field and model studies, Atmos. Chem. Phys., 11, 11069-11102,
413      10.5194/acp-11-11069-2011, 2011.

414 Faust, B. C., Powell, K., Rao, C. J., and Anastasio, C.: Aqueous-phase photolysis of biacetyl (An α-dicarbonyl
415      compound): A sink for biacetyl, and a source of acetic acid, peroxyacetic acid, hydrogen peroxide, and the
416      highly oxidizing acetylperoxyl radical in aqueous aerosols, fogs, and clouds, Atmospheric Environment, 31,
417      497-510, 1997.

418 Feng, Y. L., Wen, S., Wang, X. M., Sheng, G. Y., He, Q. S., Tang, J. H., and Fu, J. M.: Indoor and outdoor
419      carbonyl compounds in the hotel ballrooms in Guangzhou, China, Atmospheric Environment, 38, 103-112,
420      10.1016/j.atmosenv.2003.09.061, 2004.

Fu, T-M., Jacob, D. J., Wittrock, F., Burrows, J. P., Vrekoussis, M., and Henze, D. K., Global budgets of atmospheric glyoxal and methylglyoxal, and implications for formation of secondary organic aerosols, J. Geophys. Res, 113, 1-17, 2008.

Fu, T-M., Jacob, D. J., and Heald, C. L., Aqueous-phase reactive uptake of dicarbonyls as a source of organic aerosol over eastern North America, Atmos. Environ., 43, 1814–1822, 2009.

Gligorovski, S., and Herrmann, H.: Kinetics of reactions of OH with organic carbonyl compounds in aqueous solution, Phys. Chem. Chem. Phys., 6, 4118-4126, 10.1039/b403070b, 2004.

Glowa, G., Driver, P., and Wren, J. C.: Irradiation of MEK - II: A detailed kinetic model for the degradation under of 2-butanone in aerated aqueous solutions steady-state gamma-radiolysis conditions, Radiat. Phys. Chem., 58, 49-68, 10.1016/s0969-806x(99)00360-6, 2000.

Goldan, P. D., Kuster, W. C., Fehsenfeld, F. C., and Montzka, S. A.: Hydrocarbon measurements in the southeastern United States: The Rural Oxidants in the Southern Environment (ROSE) program 1990, Journal of Geophysical Research-Atmospheres, 100, 25945-25963, 10.1029/95jd02607, 1995.

Goldstein, A. H., and Galbally, I. E.: Known and unexplored organic constituents in the earth's atmosphere, Environmental Science & Technology, 41, 1514-1521, 10.1021/es072476p, 2007.

Grosjean, D.: Formaldehyde and other carbonyls in Los-Angeles ambient air, Environmental Science & Technology, 16, 254-262, 10.1021/es00099a005, 1982.

Grosjean, D., Swanson, R. D., and Ellis, C.: Carbonyls in Los-Angeles air - contribution of direct emissions and photochemistry, Sci. Total Environ., 29, 65-85, 10.1016/0048-9697(83)90034-7, 1983.

Grosjean, D., and Wright, B.: Carbonyls in urban fog, ice fog, cloudwater and rainwater, Atmospheric Environment, 17, 2093-2096, 10.1016/0004-6981(83)90368-2, 1983.

Grosjean, D., Grosjean, E., and Moreira, L. F. R.: Speciated ambient carbonyls in Rio de Janeiro, Brazil, Environmental Science & Technology, 36, 1389-1395, 10.1021/es0111232, 2002.

Hallquist, M., Wenger, J. C., Baltensperger, U., Rudich, Y., Simpson, D., Claeys, M., Dommen, J., Donahue, N. M., George, C., Goldstein, A. H., Hamilton, J. F., Herrmann, H., Hoffmann, T., Iinuma, Y., Jang, M., Jenkin, M. E., Jimenez, J. L., Kiendler-Scharr, A., Maenhaut, W., McFiggans, G., Mentel, T. F., Monod, A., Prevot, A. S. H., Seinfeld, J. H., Surratt, J. D., Szmigielski, R., and Wildt, J.: The formation, properties and impact of secondary organic aerosol: current and emerging issues, Atmos. Chem. Phys., 9, 5155-5236, 2009.

Herrmann, H., Ervens, B., Nowacki, P., Wolke, R., and Zellner, R.: A chemical aqueous phase radical mechanism for tropospheric chemistry, Chemosphere, 38, 1223-1232, 10.1016/s0045-6535(98)00520-7, 1999.

Herrmann, H., Tilgner, A., Barzaghi, P., Majdik, Z., Gligorovski, S., Poulain, L., and Monod, A.: Towards a more detailed description of tropospheric aqueous phase organic chemistry: CAPRAM 3.0, Atmospheric Environment, 39, 4351-4363, 10.1016/j.atmosenv.2005.02.016, 2005.

Herrmann, H., Schaefer, T., Tilgner, A., Styler, S. A., Weller, C., Teich, M., and Otto, T.: Tropospheric Aqueous-Phase Chemistry: Kinetics, Mechanisms, and Its Coupling to a Changing Gas Phase, Chem. Rev., 115, 4259-4334, 10.1021/cr500447k, 2015.

Isidorov, V. A., Zenkevich, I. G., and Ioffe, B. V.: Volatile organic-compounds in the atmosphere of forests, Atmospheric Environment, 19, 1-8, 10.1016/0004-6981(85)90131-3, 1985.

Kanakidou, M., Seinfeld, J. H., Pandis, S. N., Barnes, I., Dentener, F. J., Facchini, M. C., Van Dingenen, R., Ervens, B., Nenes, A., Nielsen, C. J., Swietlicki, E., Putaud, J. P., Balkanski, Y., Fuzzi, S., Horth, J., Moortgat, G. K., Winterhalter, R., Myhre, C. E. L., Tsigaridis, K., Vignati, E., Stephanou, E. G., and Wilson, J.: Organic aerosol and global climate modelling: a review, Atmos. Chem. Phys., 5, 1053-1123, 2005.

Karl, T., Chahan, Y., Jordan, A., and Lindinger, W.: Dynamic measurements of partition coefficients using proton-transfer-reaction mass spectrometry (PTR-MS), International Journal of Mass Spectrometry, 12269, 1-13, 2002.

Khalil, M. A. K., and Rasmussen, R. A.: Forest hydrocarbon emissions - relationships between fluxes and ambient concentrations, J. Air Waste Manage. Assoc., 42, 810-813, 1992.

Kirstine, W., Galbally, I., Ye, Y. R., and Hooper, M.: Emissions of volatile organic compounds (primarily oxygenated species) from pasture, Journal of Geophysical Research-Atmospheres, 103, 10605-10619, 10.1029/97jd03753, 1998.

Kroll, J. H., Ng, N. L., Murphy, S. M., Varutbangkul, V., Flagan, R. C., and Seinfeld, J. H., Chamber studies of secondary organic aerosol growth by reactive uptake of simple carbonyl compounds, J. Geophys. Res, 110, 1-10, 2005.

Lilie, J., Beck, G., and Henglein, A.: Pulse radiolysis of acetoin radicals and diacetyl anions in aqueous solution, Berichte Der Bunsen-Gesellschaft Fur Physikalische Chemie, 72, 529-&, 1968.

Lin, G., Sillman, S., Penner, J. E., and Ito, A., Global modeling of SOA: the use of different mechanisms for aqueous-phase formation, Atmos. Chem. Phys., 14, 5451–5475, 2014.

Lipari, F., Dasch, J. M., and Scruggs, W. F.: Aldehyde emissions from wood-burning fireplaces, Environmental Science & Technology, 18, 326-330, 10.1021/es00123a007, 1984.

480 Matthews, T. G., and Howell, T. C.: Visual colorimetric formaldehyde screening analysis for indoor air, Journal
481     of the Air Pollution Control Association, 31, 1181-1184, 1981.
482 Monod, A., Poulain, L., Grubert, S., Voisin, D., and Wortham, H.: Kinetics of OH-initiated oxidation of
483     oxygenated organic compounds in the aqueous phase: new rate constants, structure-activity relationships and
484     atmospheric implications, Atmospheric Environment, 39, 7667-7688, 10.1016/j.atmosenv.2005.03.019, 2005.
485 Monod, A., Chevallier, E., Jolibois, R. D., Doussin, J. F., Picquet-Varrault, B., and Carlier, P.: Photooxidation of
486     methylhydroperoxide and ethylhydroperoxide in the aqueous phase under simulated cloud droplet conditions,
487     Atmospheric Environment, 41, 2412-2426, 10.1016/j.atmosenv.2006.10.006, 2007.
488 Mopper, K., and Stahovec, W. L.: Sources and sinks of low-molecular-weight organic carbonyl-compounds in
489     seawater, Mar. Chem., 19, 305-321, 10.1016/0304-4203(86)90052-6, 1986.
490 Morillon, V., Debeaufort, F., Jose, J., Tharrault, J. F., Capelle, M., Blond, G., and Voilley, A.: Water vapour
491     pressure above saturated salt solutions at low temperatures, Fluid Phase Equilib., 155, 297-309,
492     10.1016/s0378-3812(99)00009-6, 1999.
493 Müller, K., van Pinxteren, D., Plewka, A., Svrcina, B., Kramberger, H., Hofmann, D., Bachmann, K., and
494     Herrmann, H.: Aerosol characterisation at the FEBUKO upwind station Goldlauter (II): Detailed organic
495     chemical characterisation, Atmospheric Environment, 39, 4219-4231, 10.1016/j.atmosenv.2005.02.008, 2005.
496 Pastina, B., and LaVerne, J. A.: Effect of molecular hydrogen on hydrogen peroxide in water radiolysis, J. Phys.
497     Chem. A, 105, 9316-9322, 10.1021/jp012245j, 2001.
498 Riemer, D., Pos, W., Milne, P., Farmer, C., Zika, R., Apel, E., Olszyna, K., Kliendienst, T., Lonneman, W.,
499     Bertman, S., Shepson, P., and Starn, T.: Observations of nonmethane hydrocarbons and oxygenated volatile
500     organic compounds at a rural site in the southeastern United States, Journal of Geophysical Research-
501     Atmospheres, 103, 28111-28128, 10.1029/98jd02677, 1998.
502 Rodigast, M., Mutzel, A., Iinuma, Y., Haferkorn, S., and Herrmann, H.: Characterisation and optimisation of a
503     sample preparation method for the detection and quantification of atmospherically relevant carbonyl
504     compounds in aqueous medium, Atmos. Meas. Tech., 8, 2409-2416, 10.5194/amt-8-2409-2015, 2015.
505 Schaefer, T., Schindelka, J., Hoffmann, D., and Herrmann, H.: Laboratory Kinetic and Mechanistic Studies on
506     the OH-Initiated Oxidation of Acetone in Aqueous Solution, J. Phys. Chem. A, 116, 6317-6326,
507     10.1021/jp2120753, 2012.
508 Schütze, M., and Herrmann, H.: Uptake of acetone, 2-butanone, 2,3-butanedione and 2-oxopropanal on a water
509     surface, Phys. Chem. Chem. Phys., 6, 965-971, 10.1039/b313474a, 2004.
510 Sebbar, N., Bozzelli, J. W., and Bockhorn, H.: Thermochemistry and Kinetics for 2-Butanone-1-yl Radical ($CH_2$
511     center dot $C(=O)CH_2CH_3$) Reactions with $O_2$, J. Phys. Chem. A, 118, 21-37, 10.1021/jp408708u, 2014.
512 Sebbar, N., Bozzelli, J. W., and Bockhorn, H.: Reactivity, thermochemistry and kinetics of 2-butanone radicals:
513     $CH_2C(=O)CHCH_3$, $CH_3C(=O)CHCH_3$ and $CH_3C(=O)CH_2CH_2$, 2011.
514 Sempere, R., and Kawamura K.: Comparative distribution of dicarboxylic acids and related polar compounds in
515     snow, rain and aerosols from urban, Atmos. Environ., 28, 449-459, 1994.
516 Singh, H. B., Salas, L. J., Chatfield, R. B., Czech, E., Fried, A., Walega, J., Evans, M. J., Field, B. D., Jacob, D.
517     J., Blake, D., Heikes, B., Talbot, R., Sachse, G., Crawford, J. H., Avery, M. A., Sandholm, S., and Fuelberg,
518     H.: Analysis of the atmospheric distribution, sources, and sinks of oxygenated volatile organic chemicals based
519     on measurements over the Pacific during TRACE-P, Journal of Geophysical Research-Atmospheres, 109, 20,
520     10.1029/2003jd003883, 2004.
521 Snider, J. R., and Dawson, G. A.: Tropospheric light alcohols, carbonyls and acetonitrile - concentrations in
522     southwestern united-states and henry law data, Journal of Geophysical Research-Atmospheres, 90, 3797-3805,
523     10.1029/JD090iD02p03797, 1985.
524 Stefan, M. I., and Bolton, J. R.: Reinvestigation of the acetone degradation mechanism in dilute aqueous solution
525     by the UV/H2O2 process, Environmental Science & Technology, 33, 870-873, 10.1021/es9808548, 1999.
526 Tan, Y., Carlton, A. G., Seitzinger, S. P., and Turpin, B. J.: SOA from methylglyoxal in clouds and wet aerosols:
527     Measurement and prediction of key products, Atmospheric Environment, 44, 5218-5226,
528     10.1016/j.atmosenv.2010.08.045, 2010.
529 van Pinxteren, D., Plewka, A., Hofmann, D., Muller, K., Kramberger, H., Svrcina, B., Bachmann, K., Jaeschke,
530     W., Mertes, S., Collett, J. L., and Herrmann, H.: Schmucke hill cap cloud and valley stations aerosol
531     characterisation during FEBUKO (II): Organic compounds, Atmospheric Environment, 39, 4305-4320,
532     10.1016/j.atmosenv.2005.02.014, 2005.
533 von Sonntag, C., and Schuchmann, H. P.: Aufklärung von Peroxyl-Radikalreaktionen in wäßriger Lösung mit
534     strahlenchemischen Techniken, Angew. Chem., 130, 1255-1279, 1991.
535 von Sonntag, C., and Schuchmann, H. P.: Bimolecular Decay of peroxyl radicals, in: Peroxyl radicals, edited by:
536     Alfassi, Z. B., John Wiley & sons, 199-207, 1997.
537 Ware, G. W.: Methyl ethyl ketone, Reviews of Environmental Contamination and Toxicology, 106, 165-174,
538     1988.

539 Warneke, C., Karl, T., Judmaier, H., Hansel, A., Jordan, A., Lindinger, W., and Crutzen, P. J.: Acetone, methanol,
540     and other partially oxidized volatile organic emissions from dead plant matter by abiological processes:
541     Significance for atmospheric HOx chemistry, Glob. Biogeochem. Cycle, 13, 9-17, 10.1029/98gb02428, 1999.
542 Yokelson, R. J., Burling, I. R., Gilman, J. B., Warneke, C., Stockwell, C. E., de Gouw, J., Akagi, S. K., Urbanski,
543     S. P., Veres, P., Roberts, J. M., Kuster, W. C., Reardon, J., Griffith, D. W. T., Johnson, T. J., Hosseini, S.,
544     Miller, J. W., Cocker, D. R., Jung, H., and Weise, D. R.: Coupling field and laboratory measurements to
545     estimate the emission factors of identified and unidentified trace gases for prescribed fires, Atmos. Chem.
546     Phys., 13, 89-116, 10.5194/acp-13-89-2013, 2013.
547 Zegota, H., Schuchmann, M. N., Schulz, D., and Vonsonntag, C.: Acetonylperoxyl radicals, $CH_3COCH_2O_2$ - a
548     study on the gamma-radiolysis and pulse-radiolysis of acetone in oxygenated aqueous-solutions,
549     Z.Naturforsch.(B), 41, 1015-1022, 1986.
550 Zhao, J., Levitt, N. P., Zhang, R., and Chen, J., Heterogeneous Reactions of Methylglyoxal in Acidic Media:
551     Implications for Secondary Organic Aerosol Formation, Environ. Sci. Technol., 40, 7682-7687, 2006.
552 Zhou, X. L., and Mopper, K.: Apparent partition-coefficients of 15 carbonyl-compounds between air and seawater
553     and between air and fresh-water - implications for air sea exchange, Environmental Science & Technology,
554     24, 1864-1869, 10.1021/es00082a013, 1990.
555 Zhou, X. L., and Mopper, K.: Photochemical production of low-molecular-weight carbonyl compounds in
556     seawater and surface microlayer and their air-sea exchange, Mar. Chem., 56, 201-213, 10.1016/s0304-
557     4203(96)00076-x, 1997.

Table 1: Conducted experiments in the bulk reactor.

| Number of experiment | Type of experiment | Concentration precursor compound [mmol L$^{-1}$] | Concentration H$_2$O$_2$ [mmol L$^{-1}$] | UV light ($\lambda$ = 254 nm) | Reaction time [hours] | Number of repetition |
|---|---|---|---|---|---|---|
| 1 | Oxidation of MEK | 0.1 | 2 | ✓ | 4 | 3 |
| 2 | Reaction of H$_2$O$_2$ with MEK | 0.1 | 2 | - | 4 | 1 |
| 3 | Photolysis of MEK | 0.1 | - | ✓ | 4 | 1 |
| 4 | Photolysis of H$_2$O$_2$ | - | 2 | ✓ | 4 | 1 |
| 5 | Oxidation of 2,3-butanedione | 0.1 | 2 | ✓ | 4 | 1 |
| 6 | Oxidation of hydroxyacetone | 0.1 | 2 | ✓ | 4 | 1 |
| 7 | Photolysis of 2,3-butanedione, hydroxyacetone, methylglyoxal | 0.1 | - | ✓ | 4 | 1 |

MEK: Methyl ethyl ketone
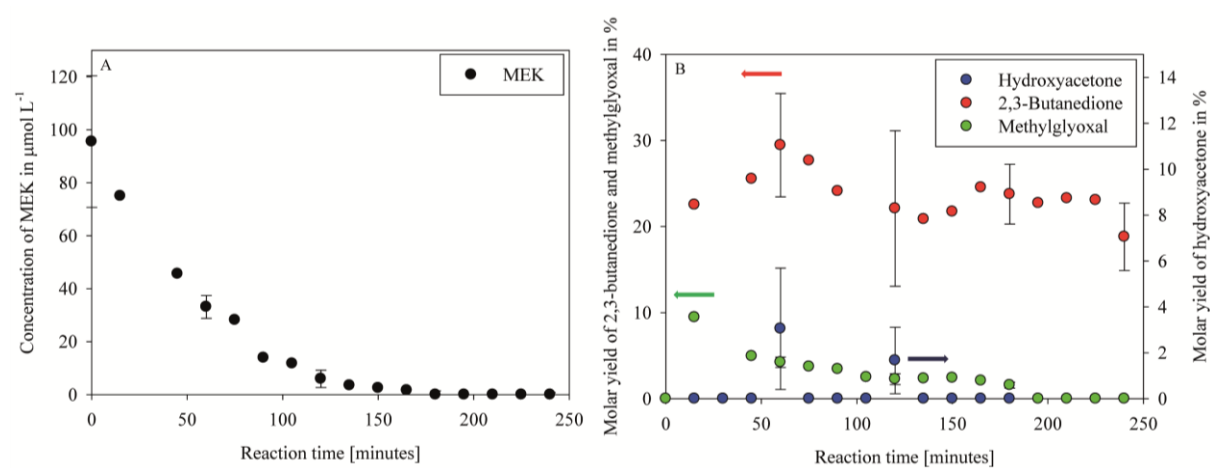


Figure 1: Consumption of MEK (A) during the oxidation with OH radicals and time-resolved formation of the products methylglyoxal (B), 2,3-butanedione (B), and hydroxyacetone (B).
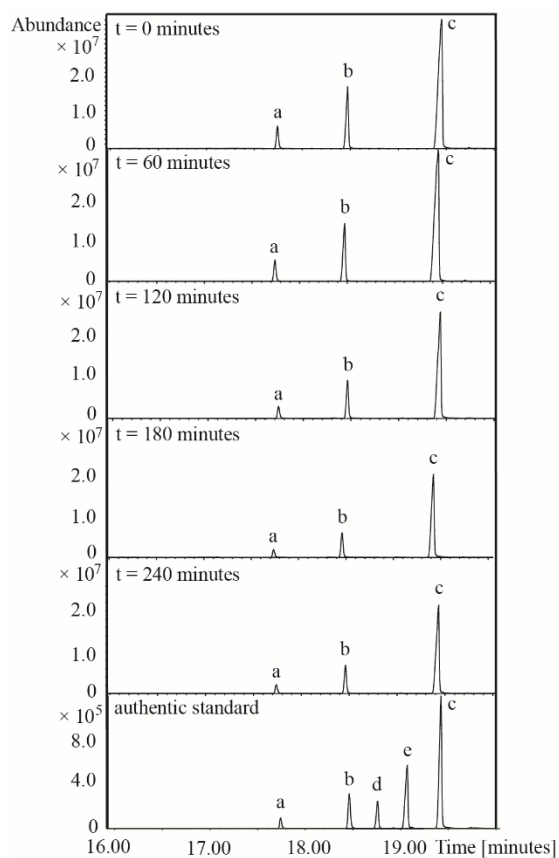
Figure 2: GC/MS chromatogram of oxidation of 2,3-butanedione (a,b,c) and the authentic standard compounds 2,3-butanedione (a,b,c) and methylglyoxal (d,e).
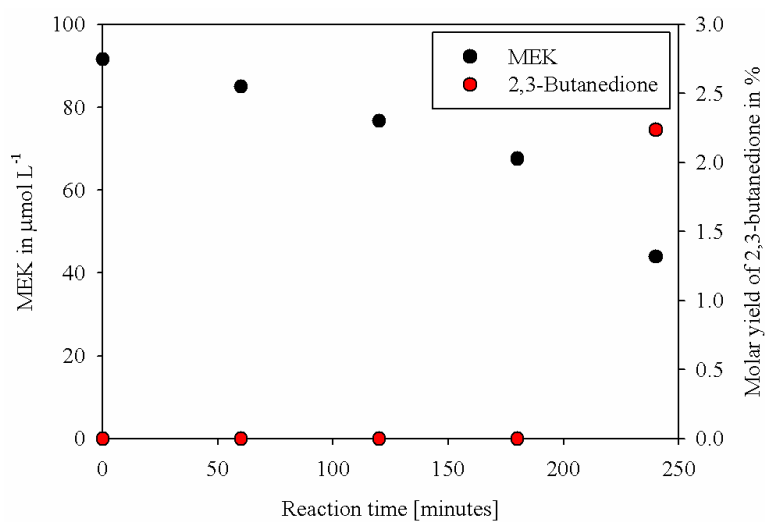


Figure 3: Photolysis of MEK and time-resolved formation of 2,3-butanedione.

Table 2: Maximal molar yields of the oxidation products.

| Oxidation product | Maximal molar yield (± standard deviation) in % | Reaction time in minutes |
|---|---|---|
| 2,3-Butanedione | 29.5 ± 6.0 | 60 |
| Methylglyoxal | 9.5 | 15 |
| Hydroxyacetone | 3.0 ± 2.6 | 60 |
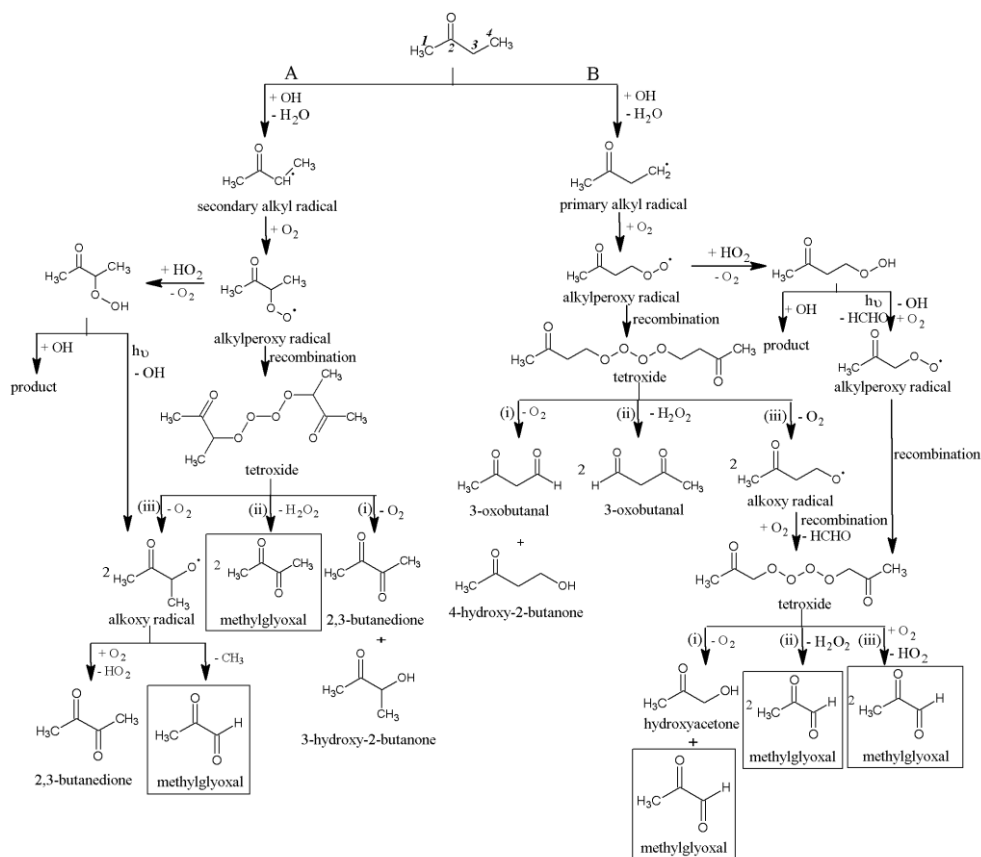


Figure 4: Recommendation of an oxidation mechanism of MEK for the formation of 2,3-butanedione, hydroxyacetone and methylglyoxal.

1

Table 3: Reaction mechanism and rate constants for the modelling of the experiment with COPASI.

| | Reaction | Rate constant k | Comment |
|---|---|---|---|
| R1 | $H_2O_2 + h\upsilon \rightarrow 2\ OH$ | $7.6 \times 10^{-6}\ s^{-1}$ | measured |
| R2 | $2\ OH \rightarrow H_2O_2$ | $3.6 \times 10^{9}\ M^{-1}\ s^{-1}$ | Elliot and Buxton, 1992 |
| R3 | $OH + H_2O_2 \rightarrow HO_2 + H_2O$ | $2.7 \times 10^{7}\ M^{-1}\ s^{-1}$ | Christensen et al., 1982 |
| R4 | $OH + HO_2 \rightarrow H_2O + O_2$ | $6 \times 10^{9}\ M^{-1}\ s^{-1}$ | Elliot and Buxton, 1992 |
| R5 | $2\ HO_2 \rightarrow H_2O_2 + O_2$ | $9.8 \times 10^{5}\ M^{-1}\ s^{-1}$ | Christensen and Sehested, 1988 |
| R6 | $HO_2 + H_2O_2 \rightarrow OH + O_2 + H_2O$ | $0.5\ M^{-1}\ s^{-1}$ | Pastina and LaVerne, 2001 |
| R7 | $CH_3C(O)CH_2CH_3 + OH \rightarrow CH_3C(O)CH_2CH_2 + H_2O$ | $9 \times 10^{8}\ M^{-1}\ s^{-1}$ | changed after Gligorovski and Herrmann, 2004 |
| R8 | $CH_3C(O)CH_2CH_3 + OH \rightarrow CH_3C(O)CHCH_3 + H_2O$ | $6 \times 10^{8}\ M^{-1}\ s^{-1}$ | changed after Gligorovski and Herrmann, 2004 |
| R9 | $CH_3C(O)CH_2CH_2 + O_2 \rightarrow CH_3C(O)CH_2CH_2O_2$ | $3.1 \times 10^{9}\ M^{-1}\ s^{-1}$ | Zegota et al., 1986 |
| R10 | $2\ CH_3C(O)CH_2CH_2O_2 + O_2 \rightarrow CH_3C(O)CH_2O_2 + 2\ HCHO$ | $4 \times 10^{7}\ M^{-1}\ s^{-1}$ | Zegota et al., 1986 |
| R11 | $2\ CH_3C(O)CH_2O_2 \rightarrow CH_3C(O)CH_2OH + CH_3C(O)C(O)H + O_2$ | $2 \times 10^{8}\ M^{-1}\ s^{-1}$ | Zegota et al., 1986 |
| R12 | $2\ CH_3C(O)CH_2O_2 \rightarrow 2\ HO_2 + 2\ CH_3C(O)C(O)H$ | $4 \times 10^{7}\ M^{-1}\ s^{-1}$ | Zegota et al., 1986 |
| R13 | $2\ CH_3C(O)CH_2O_2 \rightarrow 2\ CH_3C(O)C(O)H + H_2O_2$ | $4 \times 10^{8}\ M^{-1}\ s^{-1}$ | Zegota et al., 1986 |
| R14 | $CH_3C(O)CH_2CH_2O_2 + HO_2 \rightarrow CH_3C(O)CH_2CH_2OOH + O_2$ | $1 \times 10^{7}\ M^{-1}\ s^{-1}$ | Von Sonntag and Schuchmann, 1991 |
| R15 | $CH_3C(O)CH_2CH_2OOH + OH \rightarrow Product$ | $2.7 \times 10^{7}\ M^{-1}\ s^{-1}$ | Christensen et al., 1982 |
| R16 | $CH_3C(O)CH_2CH_2OOH \rightarrow OH + HCHO + CH_3C(O)CH_2$ | $7.6 \times 10^{-7}\ s^{-1}$ | after Monod et al., 2007 |
| R17 | $CH_3C(O)CH_2 + O_2 \rightarrow CH_3C(O)CH_2O_2$ | $3.1 \times 10^{9}\ M^{-1}\ s^{-1}$ | Zegota et al., 1986 |
| R18 | $2\ CH_3C(O)CH_2O_2 \rightarrow CH_3C(O)CH_2OH + CH_3C(O)C(O)H + O_2$ | $2 \times 10^{8}\ M^{-1}\ s^{-1}$ | Zegota et al., 1986 |
| R19 | $2\ CH_3C(O)CH_2O_2 \rightarrow H_2O_2 + 2\ CH_3C(O)C(O)H$ | $4 \times 10^{8}\ M^{-1}\ s^{-1}$ | Zegota et al., 1986 |
| R20 | $2\ CH_3C(O)CH_2O_2 \rightarrow 2\ CH_3C(O)C(O)H + HO_2$ | $4 \times 10^{7}\ M^{-1}\ s^{-1}$ | Zegota et al., 1986 |
| R21 | $CH_3C(O)CHCH_3 + O_2 \rightarrow CH_3C(O)CHO_2CH_3$ | $3.1 \times 10^{9}\ M^{-1}\ s^{-1}$ | Glowa et al., 2000 |
| R22 | $2\ CH_3C(O)CHO_2CH_3 \rightarrow O_2 + CH_3C(O)C(O)CH_3 + CH_3C(O)CHCH_3OH$ | $2.5 \times 10^{8}\ M^{-1}\ s^{-1}$ | Glowa et al., 2000 |
| R23 | $2\ CH_3C(O)CHO_2CH_3 \rightarrow H_2O_2 + 2\ CH_3C(O)C(O)CH_3$ | $4.5 \times 10^{8}\ M^{-1}\ s^{-1}$ | Glowa et al., 2000 |
| R24 | $2\ CH_3C(O)CHO_2CH_3 \rightarrow CH_3C(O)C(O)CH_3 + CH3C(O)C(O)H + CH_3 + HO_2$ | $5 \times 10^{7}\ M^{-1}\ s^{-1}$ | Glowa et al., 2000 |
| R25 | $CH_3C(O)CHO_2CH_3 + HO_2 \rightarrow CH_3C(O)CHOOHCH_3 + O_2$ | $1 \times 10^{7}\ M^{-1}\ s^{-1}$ | Von Sonntag and Schuchmann, 1991 |
| R26 | $CH_3C(O)CHOOHCH_3 \rightarrow CH_3C(O)CHOCH_3 + OH$ | $7.6 \times 10^{-7}\ s^{-1}$ | after Monod et al., 2007 |
| R27 | $2\ CH_3C(O)CHOCH_3 \rightarrow CH_3C(O)C(O)H + CH_3C(O)C(O)CH_3 + CH_3 + HO_2$ | $4 \times 10^{7}\ M^{-1}\ s^{-1}$ | Zegota et al., 1986 |
| R28 | $CH_3C(O)CHOOHCH_3 + OH \rightarrow Product$ | $2.7 \times 10^{7}\ M^{-1}\ s^{-1}$ | Christensen et al., 1982 |
| R29 | $CH_3C(O)C(O)H + OH \rightarrow Product$ | $5.3 \times 10^{8}\ M^{-1}\ s^{-1}$ | Monod et al., 2005 |
| R30 | $CH3C(O)C(O)H \rightarrow Product$ | $3 \times 10^{-5}\ s^{-1}$ | measured |
| R31 | $CH_3C(O)C(O)CH_3 + OH \rightarrow Product$ | $1.4 \times 10^{8}\ M^{-1}\ s^{-1}$ | Gligorovski and Herrmann, 2004 |
| R32 | $CH_3C(O)C(O)CH_3 \rightarrow Product + 0.17\ CH_3C(O)C(O)H$ | $9 \times 10^{-6}\ s^{-1}$ | measured |
| R33 | $CH_3C(O)CH_2OH + OH \rightarrow CH_3C(O)C(O)H$ | $8 \times 10^{8}\ M^{-1}\ s^{-1}$ | Stefan and Bolton, 1999 |
| R34 | $CH3C(O)CH_2OH \rightarrow Product + 0.19\ CH_3C(O)C(O)H$ | $2 \times 10^{-5}\ s^{-1}$ | measured |
| R35 | $CH_3C(O)CH_2CH_3 \rightarrow Product + 0.02\ CH_3C(O)C(O)CH_3$ | $5 \times 10^{-5}\ s^{-1}$ | measured |
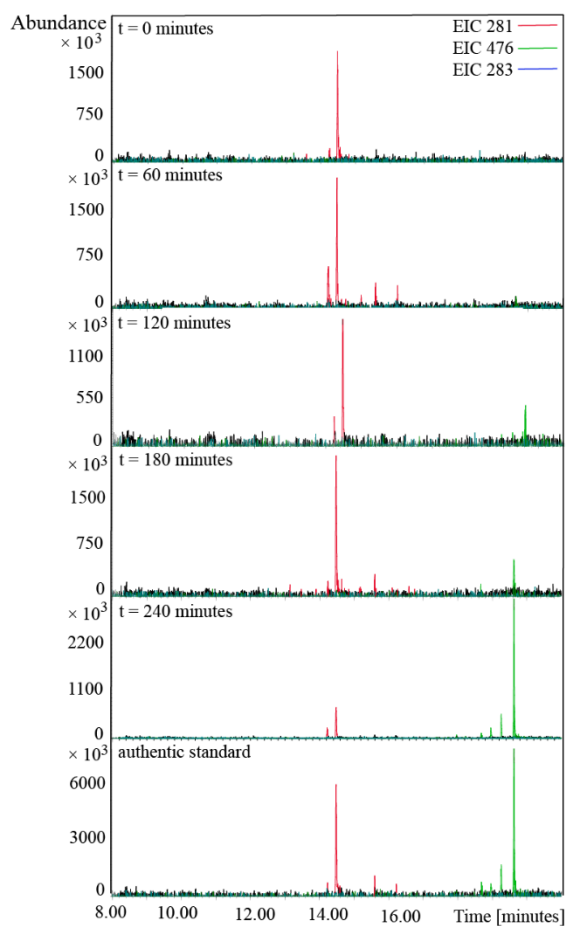
Figure 5: Extracted ion chromatogram (EIC) of *m/z* 281 M$^{\bullet+}$, *m/z* 476 M$^{\bullet+}$ and *m/z* 283 M$^{\bullet+}$ during the oxidation of MEK and EIC of the authentic standard compounds.
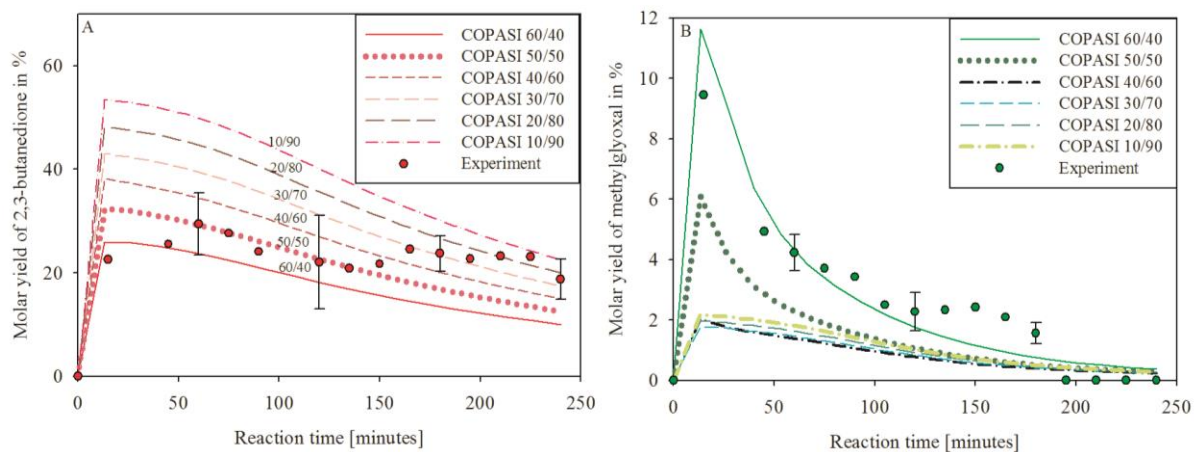


Figure 6: Comparison of the molar yields of 2,3-butanedione (A) and methylglyoxal (B) for the model and experimental results using different branching ratios of the primary/secondary H-atom abstraction varied between 60/40 up to 10/90.
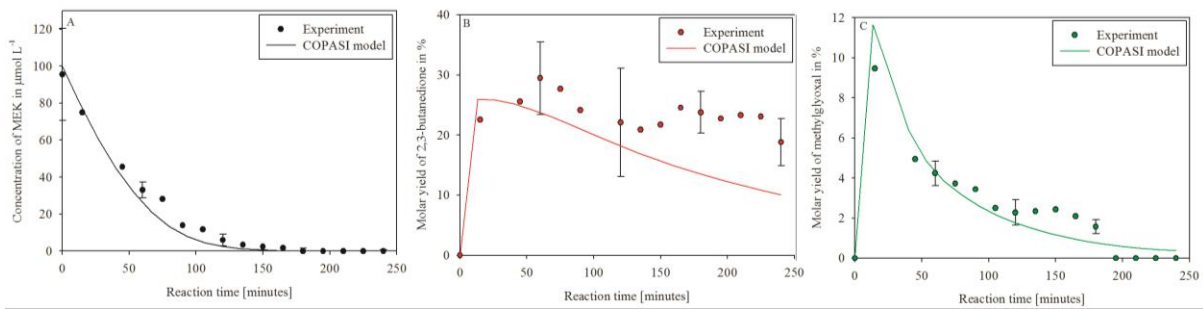
Figure 7: Comparison of the model and experimental results for MEK (A), 2,3-butanedione (B), and methylglyoxal (C).